Paper III

Wiedmann I, Reigstad M, Marquardt M, Vader A, Gabrielsen T M

Seasonality of vertical flux and sinking particle characteristics in an ice-free high Arctic fjord – different from sub-Arctic fjords?

Submitted after revision to *Journal of Marine Systems*.

Seasonality of vertical flux and sinking particle characteristics in an ice-free high Arctic fjord – different from sub-Arctic fjords?

Ingrid Wiedmann (1)
Marit Reigstad (1)
Miriam Marquardt (1, 2)
Anna Vader (2)
Tove M. Gabrielsen (2)

(1) UiT The Arctic University of Norway, Breivika, 9037 Tromsø, Norway
(2) The University Centre in Svalbard (UNIS), 9171 Longyearbyen, Norway

Corresponding author:
Ingrid Wiedmann
UiT The Arctic University of Norway
9037 Tromsø
Norway
Email: Ingrid.Wiedmann@uit.no
Tel.: 0047 776 44214

Abstract

Seasonality in plankton dynamics is strongly affected by sea ice cover and light regime in the Arctic. The Arctic Adventfjorden (78 °N, 15 °E, western Svalbard) was previously seasonally ice-covered, but has tended to be ice-free since 2007. It may accordingly serve as a model area to study the vertical flux in a year-round ice-free Arctic fjord. We investigated (1) how the vertical flux of organic matter follows the seasonal pattern of suspended material, (2) how sinking particles' characteristics change with seasons and are linked to the vertical flux, and (3) if the vertical flux in an Arctic but ice-free fjord with a major glacial run-off during autumn is comparable to boreal and sub-Arctic ice-free fjords. We conducted seven field samplings between December 2011 and September 2012, measuring the suspended biomass (chlorophyll *a*, particulate organic carbon) at 5, 15, 25 and 60 m and the vertical biomass flux (short-term sediment traps for 24 h; 20, 30, 40, 60 m). Sediment traps modified with gel-filled jars were deployed to study sinking particles' characteristics (size and frequency distribution, particle type). The resuspension from the seafloor by winter wind mixing and thermal convection resulted in large, detrital sinking particles. Intense biomass sedimentation (fresh to little degraded biomass) was found during the early spring bloom but diminished toward the late bloom phase. The highest flux of particulate organic carbon (POC) was found during autumn (770-1530 mg POC m^{-2} d^{-1}), when sediment loaded glacial run-off and high pteropod abundances were observed. The vertical carbon flux in the Arctic Adventfjorden appears to resemble sub-Arctic fjords during winter and spring, but during autumn, a pulsed major POC flux may be induced by glacial run-off.

(277 words)

Keywords

- Gel trap
- Particulate organic carbon (POC)
- Particle size spectra
- Aggregate
- Detritus
- Glacial run-off

Highlights

- Ice-free Adventfjorden resembled sub-Arctic fjords during winter and spring
- Two major annual sedimentation events in ice-free Adventfjorden, Svalbard
- Highly variable POC: volume ratio due to different particle types and seasons
- High autumn POC flux associated with glacial run-off

1 Introduction

Strong seasonality in high latitude marine ecosystems generates an oscillating annual pattern of nutrient concentrations as well as phytoplankton and zooplankton abundance throughout the year (Leu et al., 2011; Rat'kova and Wassmann, 2002; Węsławski et al., 1991). This, in turn, is presumed to determine the quality and intensity of the vertical biomass flux (De La Rocha and Passow, 2007; Peinert et al., 1989; Wassmann et al., 1991), but few field studies thus far have examined how sinking particles' characteristics change with seasons and how they may be linked to the vertical carbon flux during different seasons (e.g., Mackenzie Shelf, Forest et al., 2013).

It has been postulated that fjords are areas of enhanced organic carbon sequestration (Smith et al., 2015). The major vehicle of the vertical carbon flux are algal aggregates, fecal pellets detritus and marine snow, i.e. conglomerates (> 0.5 mm) of diverse composition and structure (Alldredge and Silver, 1988).

Ice algae tend to form blooms in seasonally ice-covered fjords in April-May (Ji et al., 2013; Leu et al., 2011). Heterotrophs, such as the copepod *Calanus glacialis*, utilize these blooms (Søreide et al., 2010; Weydmann et al., 2013), but ice algal biomass also contributes to the vertical export, when the cells are released into the water column during ice break-up (Arrigo, 2014; Tremblay et al., 1989).

Phytoplankton spring blooms occur in ice-free fjords in April and May and in seasonally ice-covered fjords subsequent to the ice break-up (Eilertsen and Frantzen, 2007; Leu et al., 2011). Diatoms, a prominent spring bloom taxon in high latitudes, can cause major biomass sedimentation (Thompson et al., 2008; Wassmann et al., 1991). Their senescent cells and resting stages have high sinking velocities (Rynearson et al., 2013; Smayda, 1971), and some taxa release sticky exopolymeric substances, which contribute to the formation of algal aggregates (Kiørboe et al., 1994; Thornton, 2002) and marine snow (Alldredge and Silver, 1988; Lampitt, 2001). Coagulation of single cells into aggregates or marine snow increases the particle size, which, in turn, enhances the sinking velocity and the vertical export of organic carbon.

However, the prymnesiophyte *Phaeocystis pouchetii* can also dominate the phytoplankton blooms in the Barents Sea and the waters around Svalbard (Degerlund and Eilertsen, 2010). This small flagellate has a low sinking velocity, and high cell abundances of this species appear to diminish the vertical carbon flux below 60 m (Reigstad and Wassmann, 2007; Reigstad et al., 2000).

Irrespective of the phytoplankton composition, an enhanced vertical carbon flux only occurs, when the zooplankton community in the fjords executes a weak top-down regulation, allowing sinking of ungrazed biomass. Top-down regulation by zooplankton reduces the vertical biomass flux by grazing and some taxa, such as copepods, also fragment sinking particles into smaller, slowly sinking material (Noji et al., 1991; Svensen et al., 2012). Alternatively, copepods and krill also enhance the vertical carbon flux by re-packaging small particles into fast sinking fecal pellets (Turner, 2002; Turner, 2015; Wexels Riser et al., 2008).

Glacial run-off entrains lithogenic material with a high specific weight. When sinking particles 'scavenge' this material, the sinking velocity of the organic material increases and enhances the vertical biomass flux (Passow and De La Rocha, 2006).

In the present study, we conducted a nine-month field study in the Arctic Adventfjorden (78 °N, 15 °E, Fig. 1), western Svalbard. Previously, the fjord was seasonally ice-covered, but it has mostly been ice-free since 2007 (www.met.no). Adventfjorden may therefore serve as a model area to study the mechanisms of vertical flux in an ice-free, but glacially influenced Arctic fjord. Our aim was to investigate: (1) how the vertical flux of organic matter follows the seasonal pattern of suspended material; (2) how sinking particles' characteristics change with season and are linked to the vertical flux, and (3) if the vertical flux in an ice-free Arctic fjord with a major glacial run-off during autumn, is comparable the vertical flux in boreal and sub-Arctic ice-free fjords.

2 Materials and methods

2.1 Study site and sampling program

The present study was conducted at station IsA (Isfjorden-Adventfjorden, 78 ° 15.67' N, 15 ° 32.10' E, Fig. 1) in the mouth of the Arctic Adventfjorden. Adventfjorden is a ~8 km long, 3.5 km wide and < 100 m deep side branch of Isfjorden, a large fjord system on the western coast of Svalbard. Neither Isfjorden nor Adventfjorden has a sill at the fjord-mouth, and they are therefore exposed to advection from the Atlantic-influenced West Spitsbergen Current. Warmer and more saline water from this current reached the study site (~50 km from the open coast) and allowed year-round ship-based sampling in ice-free waters. Glacial run-off (Advent River, Longyear River, Fig. 1) affected IsA during the summer and autumn with substantial

amounts of sediment-loaded melt water (e.g. $9*10^6$ m^{-3} during September, Węsławski et al., 1999).

Field investigations were conducted throughout nine months, starting 14.12.2011 and ending 19.09.2012. We refer to the winter sampling days in December, mid-January and late January as Winter I, Winter II and Winter III, respectively (Table 1). Spring sampling days in late April, mid-May and late May are denoted as Spring I, Spring II and Spring III, respectively, and the mid-September sampling is denoted as Autumn I (Table 1).

2.2 Hydrography, light and wind data

Hydrographical data included temperature and salinity measurements by a CTD (SD204, SAIV A/S, Bergen, Norway) and subsequent computation of the potential density. The seasonal light cycle at 78 °N includes the polar night from mid-November to late January. The sun is below the horizon from early October to early March, and the midnight sun appears between mid-April to late August. The underwater irradiance was quantified using a hand-held LI-1000 Data Logger (Li-COR, Nebraska, USA), and the euphotic zone was defined as the layer of > 1 % surface irradiance. Boat drift due to strong wind events made vertical deployment of the irradiance logger difficult, and an overestimation of the euphotic zone may be assumed. Wind data from Longyearbyen airport (78 ° 14' N, 15 ° 28' E, Fig. 1) is considered to be representative for the IsA station and were downloaded from the Norwegian Meteorological Institute (www.eklima.met.no).

2.3 Suspended biomass (Chl *a*, POC, PON)

Sea water samples were collected at 5, 15, 25 and 60 m with a 10 L Niskin bottle, transferred into carboys, and stored dark and cool until filtration within a few hours (Table 1). Triplicates of 250-400 mL were vacuum-filtered on Whatman GF/F filters for analysis of the Chl *a* concentration. Filters were frozen in liquid nitrogen or at -80 °C until analysis within nine months. Some pigment break-down resulting from the storage period may be assumed (Mantoura et al., 1997). Chl *a* was extracted 20-24 h in 10 mL methanol (darkness, +4 °C) and concentrations were then measured in a Turner Design AU-10 fluorometer (calibrated with Chl *a*, Sigma S6144). For POC and PON analysis, triplicate subsamples (300-500 mL) were filtered on pre-combusted Whatman GF/F filters, stored at -20 °C and analyzed within 2.5 years on a Leeman Lab CHN Analyzer following the procedures described in Reigstad et al. (2008).

2.4 Vertical flux characterization (Chl *a*, POC, particle size spectra)

An anchored short-term sediment trap array was used to study the vertical flux of particulate material at IsA (Table 1). Paired trap cylinders (KC Denmark, d= 7.2 cm, 45 cm high, no bafflers or poison) were mounted at 20, 30, 40 and 60 m and deployed for ca. 24 h (Table 1). In this way, we collected particles sinking out from the lower eutrophic zone and below it (Table 1), and we minimized the sampling of re-suspended material from the seafloor (~80 m).

After the trap array recovery water from one of the paired cylinders per depth was transferred into carboys. Sub-samples were filtered to determine the vertical flux of Chl *a* and POC as described above for the suspended samples (duplicates or triplicates of 150-400 mL for Chl *a*, duplicates or triplicates of 250-500 mL for POC). The second trap cylinder at each depth was modified with a gel-containing glass jar, fitting perfectly inside the trap cylinder (conceptual idea by Lundsgaard et al., 1999; modification from polyacrylamide to commercially available unpoisonous gels by Thiele et al., 2015 and Wiedmann et al., 2014) to study the vertical flux of particles $\geq$ 50 µm ESD_{image} (estimated spherical diameter determined from images) by an image analysis (concept by Ebersbach and Trull, 2008; Wiedmann et al., 2014). The threshold function of ImageJ (AutoThresholding following Otsu clustering algorithm, Otsu, 1979) was applied to establish a border between the particle and background in the 8-bit grey converted images. Particles < 50 µm ESD_{image} were excluded due to abundance underestimation (Jackson et al., 1997; Jackson et al., 2005). The remaining particles were binned in 20 bins from 0.050 mm to 5.080 mm ESD_{image} (Table A.1) and an ellipsoidal particle shape was assumed to estimate the particle volume (Wiedmann et al., 2014). The sediment trap deployment time was adjusted for the season (Table 1). During Winter I-III, we deployed the traps for ~24 h. During spring and autumn, the trap array was first deployed for ~24 h to determine the biogeochemical flux, and then for ~2 h to study the particle flux using gel-modified cylinders (short deployment prevented particle overload in the gels).

2.5 Calculation of the loss rate and sinking velocity

The loss rate can be expressed as the ratio of the vertical flux (POC, Chl *a* at depth z) to the integrated suspended biomass (POC, Chl *a* above depth z). For the calculation of loss rates, the integrated suspended biomass was estimated by trapezoidal integration. Similarly, the average sinking velocity was expressed by the ratio of the vertical flux (mg m^{-2} d^{-1}) to the suspended biomass (mg m^{-3}) at depth z (Kiørboe et al., 1994).

3 Results

3.1 Hydrography, light regime and wind

The hydrographic environment at station IsA (Fig. 2) reflected the seasonal pattern of the region. Cooling of the entire water column took place until mid-January, when warmer, denser and more saline water from the West Spitsbergen Current was advected to the station area. Another cooling period took place in April, and resulted in low water temperatures that persisted throughout May (-0.5 to 1.0 °C). Thermal warming of the surface layers started in June, and maximum surface water temperatures were reached in late August, co-occurring with enhanced glacial melt water run-off and a freshening of the surface water layers (23.8.2012: maximum water temperature 6.4 °C, minimum salinity 31.5). Low air temperatures cooled the surface waters from September onward, while deeper water layers in the fjord were still warm until late October (< 4.1 °C, Fig. 2). As glacial run-off ceased during autumn, the surface salinity increased (Fig. 2). Light was measured from 8.3.2012 onwards, when the sun rose above the horizon. Irradiance measurements indicated an euphotic zone ranging down to 20-40 m (Table 1), with the exception of a very shallow euphotic zone of 8 m on 6.7.2012. Wind data from Longyearbyen airport (Fig. 1) showed a prevailing wind direction "out of Adventfjorden" (6 of 7 sampling periods had a wind direction of E-SSW, data not shown). The opposite wind direction ("into Adventfjorden") was only observed during Spring III.

3.2 Suspended biomass (Chl *a*, POC) and its C/N ratio

The temporal high-frequency sampling of the suspended biomass parameters Chl *a* and POC showed clear seasonal patterns (Fig. 2). The Chl *a* and POC concentrations were both low during winter, increased and peaked during the spring period (late April to end of May) and showed a decreasing trend throughout summer and autumn. These data provided a seasonal framework for our seven sampling events and indicated that Winter I-III, Spring I-III and Autumn I (Fig. 2, blue lines) were typical representatives for seasonal scenarios with low, high and intermediate suspended Chl *a* and POC concentrations, respectively. However, the vertical distribution of the suspended biomass during the sampling events (Fig. 3) indicated that there was also a distinct trend in the suspended biomass during the spring bloom.

A seasonal trend was also observed in the quality of the particulate organic material reflected through (atomic) C/N ratios. Fresh material of algal origin is expected to reflect the Redfield ratio (C/N = 6.6). During Winter II and III, C/N ratios of 8.3-12.1 indicated that the biomass in the water column consisted of partly degraded material or a mixture of fresh marine

material and biomass from terrestrial origin (terrestrial material C/ N > 17, Bianchi, 2006). Fresh organic material prevailed during Spring I-III, as indicated by C/N ratios close to the Redfield ratio. During Autumn I, C/N ratios of 8.5-10.5 indicated again either degraded marine material or a mixture of terrestrial and fresh marine material.

3.3 Vertical biomass flux (Chl *a*, POC) and its C/N ratio

The vertical flux patterns of Chl *a* and POC reflected a seasonality, partly matching the observations for the suspended material. During Winter I-III, vertical Chl *a* and POC flux were relatively low, with 90-140 mg POC m^{-2} d^{-1} and < 0.26 mg Chl *a* m^{-2} d^{-1} (Fig. 4), respectively, but indicated that biomass was sinking out during the polar night. The highest POC fluxes were measured during Winter II in the deepest traps, implying a resuspension event rather than sinking POC from the water column. The highest vertical Chl *a* fluxes were found during Spring I-II, and vertical POC fluxes also were high (>1000 mg POC m^{-2} d^{-1}). The maximum vertical POC flux (< 1500 mg POC m^{-2} d^{-1}) was found during Autumn I (Fig. 4). Generally, the loss rates of Chl *a* and POC were higher at 30 m than at 60 m (exception Winter III, Table 2). The sinking velocities, in contrast, were always higher at 60 m (Table 2). The highest POC loss rate (36 %) and sinking velocity (12 m d^{-1}) was found during Autumn I (Table 2). The C/N ratio of sinking material suggested the sedimentation of degraded material during Winter II-III and Autumn I (C/N ratio: 10-15). During Spring I-III, the sinking material had a C/N ratios similar to the suspended biomass (C/N ratio: 6-8, Table 3), suggesting a vertical flux of recently produced biomass.

3.4 Particle size and volume flux

Volume flux spectra (Fig. 5) provide information on the characteristics of sinking particles in the form of particle size (and volume) distribution and frequency. The area under the curve in the volume flux spectra corresponds to the total particle volume sinking out at a particular sampling date and depth. Our data show that the volume flux tended to be the highest at 60 m and lowest at 30 m (except during Spring III, with minimum at 20 m).

During Winter I, the largest particles were found in the 2.23 mm ESD_{image} size bin (Table A.1), and a total volume flux of 312-545*10^3 mm^{-3} m^{-2} d^{-1} was estimated for the different sediment trap depths (Fig. 5). Due to the ellipsoidal volume calculation (Wiedmann et al., 2014), the median size of the volume flux could not be given, as an ellipsoidal volume could not be converted back to one definite particle ESD_{image}. Thus, we can only state that medium and large sized particles (Fig. 5, Table A.1) contributed most to the volume flux at 30 m and

40 m during Winter I, while large particles were important at 20 m and 60 m. During Spring II, medium sized particles were important contributors to the vertical volume flux down to 40 m, but extra-large particles were also found at 60 m (4.56 mm ESD_{image} size bin). Accordingly, the volume flux spanned from 171 to 1,195*10^3 mm^{-3} m^{-2} d^{-1}. During Spring III, all of the particles were small to medium-sized and found in size bins ≤ 1.81 mm ESD_{image} (apart from one single particle at 20 m with 5.15 mm ESD_{image}), and the total volume flux was moderate with 640-736*10^3 mm^{-3} m^{-2} d^{-1} (Fig. 5). Autumn I was characterized by medium sized sinking particles (bins ≤ 1.44 mm ESD_{image}) at 20 m and 30 m. Extra-large particles (≤ 3.62 mm ESD_{image} size bin) were found at 40 and 60 m, where also the highest volume fluxes of the present study were estimated (2,148 and 6,189 *10^3 mm^{-3} m^{-2} d^{-1}, respectively, Fig. 5).

The semi-quantitative visual inspection of the gels indicated that fine, degraded detritus dominated the vertical flux during Winter I (Fig. 6). The material was accompanied by some individuals of the pteropod *Limacina* sp. (characterized as swimmers and not included in the vertical flux estimates). Detrital material was still observed in the gel deployed during Spring II, but phytoplankton aggregates were also found. Phytoplankton aggregates dominated the observed particles in the gels deployed during Spring III, but they occurred together with detritus and fecal pellets. During Autumn I, a mixture of aggregates (probably phytoplankton), fecal pellets and detritus prevailed in the gels, as well as a substantial number of *Limacina* sp. individuals (up to 138 at 20 m).

4 Discussion

Investigating the seasonality in vertical biomass flux and particle characteristics showed that some of the seasonal drivers, such as phytoplankton blooms, were similar in ice-free Arctic, sub-Arctic and boreal fjords. Glacial run-off impacted sinking particles' characteristics and provided an additional driver for the vertical carbon flux in the open Arctic Adventfjorden during the melting period.

4.1 Seasonal variation of suspended biomass in Adventfjorden – reflecting typical high latitude seasonality?

Adventfjorden, an Arctic fjord influenced by the Atlantic derived West Spitsbergen Current, showed a pronounced seasonal variation during the nine months covered by the present field study. The high frequency sampling program of hydrography and suspended biomass (Fig. 2)

297 placed our field studies within three distinct seasons - winter, spring and autumn. Each of the
298 investigation periods was categorized into one of these seasons, based on environmental and
299 ecological parameters.
300 Low irradiance and deep mixing processes (wind, thermal convection) during the polar night
301 causes light limitation and prevents production and built up of autotrophic biomass in high
302 latitudes. Therefore, our winter data (Fig. 2, 3) were typical for this season and corresponded
303 to previous observations of low biomass concentrations from Svalbard (Iversen and Seuthe,
304 2011; Zajączkowski et al., 2010), the Barents Sea (Olli et al., 2002) and northern Norway
305 (Eilertsen and Degerlund, 2010; Noji et al., 1993) during winter (Table 4).
306 The onset of the phytoplankton spring bloom took place in April in nutrient sufficient (4.5 µM
307 nitrate, Kubiszyn et al., in prep.), cold and non-stratified waters (Fig. 2), with a deep euphotic
308 zone (Table 1). This is a common situation in high latitude regions (Eilertsen, 1993;
309 Townsend et al., 1992). The early spring bloom phase has been associated with a high surface
310 concentration of phytoplankton due to low zooplankton abundances (North Atlantic: Parsons
311 and Lalli, 1988). Because we experienced this situation during Spring I in late April (Fig. 3,
312 low zooplankton abundance: ~$4*10^3$ ind. m^{-3}, E.I. Stübner, pers. comm.), the sampling period
313 was characterized as a typical representation of an early bloom.
314 Spring II in mid-May was classified as a peak bloom situation, based on high Chl *a*
315 concentrations (Fig. 2, 3). Nitrate concentrations were not depleted at 25 m, while silicate was
316 low (1.5 µM nitrate + nitrite, 0.3 µM silicate, Kubiszyn et al., in prep.). A typical spring
317 bloom phytoplankton mixture of the diatoms *Chaetoceros socialis* and *Thalassiosira*
318 *nordenskioeldii* prevailed together with the prymnesiophyte *Phaeocystis pouchetii* (Kubiszyn
319 et al., in prep.). These species represent a typical spring bloom community, as previously
320 described for northern Norway, the waters around Svalbard and the Barents Sea (Degerlund
321 and Eilertsen, 2010).
322 Nitrate is considered to be the primary limiting nutrient for primary production in the Arctic
323 (Tremblay and Gagnon, 2009), and was depleted at 25 m during Spring III in late May.
324 Additionally, silicate concentrations were still low (0.9 µM, Kubiszyn et al., in prep.). The
325 abundant and divers zooplankton community (ca. $20*10^3$ ind. m^{-3}) with 40-70 %
326 meroplanktonic nauplii and larvae (Stübner et al., submitted, E.I. Stübner pers. comm.) most
327 likely exerted a strong grazing pressure and top-down regulation on the phytoplankton,
328 restraining the suspended Chl *a* (Fig. 3). Accordingly, we classified Spring III in late May as a
329 late bloom stage.

Water-mass stratification broke down due to cooling before Autumn I in mid-September. Nutrients were replenished (2.6 µM nitrate, 2.5 µM silicate, Kubiszyn et al., in prep.), but no autumn bloom in the form of biomass build up was observed (Fig. 3). We do not have data on primary production and cannot evaluate if this was a result of low production or of high loss rates (e.g., grazing from moderately abundant zooplankton: ~7*10^3 ind. m^{-3}, Stübner et al., submitted). Autumn I was considered to be a typical representation of an autumn situation.

Zajączkowski et al. (2010) reported higher concentrations of suspended Chl *a* and POC from the innermost, shallow part of Adventfjorden (40 m, ~400 m to Advent River and Longyear River) than we found at IsA. This was probably caused by higher resuspension of previously sedimented allochthonous bottom material in the shallow innermost Adventfjorden (e.g., by thermal convection or tidal mixing, Zajączkowski et al., 2010; Zajączkowski and Włodarska-Kowalczuk, 2007). High C/N ratios (> 16) in their suspended material supports this assumption (Table 4).

Suspended biomass concentrations at IsA corresponded well with previous studies from the central Barents Sea (Olli et al., 2002), western Svalbard (Kongsfjorden, Iversen and Seuthe, 2011), northern Norway (Balsfjorden/ Malangen, Eilertsen and Degerlund, 2010; Ramfjorden, Noji et al., 1993; Balsfjorden, Reigstad and Wassmann, 1996; Malangen, Wassmann et al., 1996), western Norway (Fanafjorden, Wassmann, 1984) and Conception Bay, Canada (Thompson et al., 2008, Table 4). The variability in bloom magnitude reported in the literature (e.g., present study: 0.6-4.2 mg Chl *a* m^{-3}; Kongsfjorden, western Svalbard, Iversen and Seuthe, 2011: 0.2-10 mg Chl *a* m^{-3}) most likely reflected our coarser temporal sampling resolution, which may have missed the bloom maximum.

In conclusion, we assume that the seasonal variation of suspended biomass at IsA reflected the typical high latitude seasonality. The timing of the bloom in April/ May in the fjords seem to be comparable across latitudes from sub-Arctic to Arctic ice-free fjords, while bloom conditions in May were reported for the Barents Sea and Conception Bay, Canada (Olli et al., 2002; Thompson et al., 2008).

4.2 Seasonality of the vertical flux intensity (POC, Chl *a*) in Adventfjorden – congruent with other ice-free high latitude regions?

Vertical flux intensity is determined by the overlaying processes of hydrography, phytoplankton and zooplankton. Short-term sediment traps can be used to estimate the vertical Chl *a* and POC flux and give insight into sinking particles' characteristics and, in combination

with suspended biomass data, into the vertical flux regulation during the time of deployment. However, short-term traps deployed for ~24 h only give a snap-shot picture and cannot provide robust seasonal or annual flux patterns. A comparison with previous published data was conducted to evaluate if the vertical flux seasonality at IsA was comparable to the seasonal flux pattern of other ice-free high latitude regions.

Chl *a* and POC fluxes at IsA during winter were comparable to literature data from the innermost part of Adventfjorden (Zajączkowski et al., 2010), Ramfjorden (northern Norway, Noji et al., 1993), Fanafjorden (western Norway, Wassmann, 1984) and the open Barents Sea (Olli et al., 2002; Table 4). Some differences between the two studies in Adventfjorden (present study: 90-400 mg POC m^{-2} d^{-1}; Zajaczkowski et al., (2010): < 750 mg POC m^{-2} d^{-1}; Table 4) seem to reflect the resuspension of bottom material in the shallow parts of the fjord (as observed for the suspended material), and the C/N ratios of up to 25 in the sinking material clearly reflected terrestrial input (Zajączkowski et al., 2010).

Our strong pulses of vertical Chl *a* and POC flux during the spring exceeded previous measurements from the innermost Adventfjorden (Zajączkowski et al., 2010), Balsfjorden and Malangen (northern Norway, Keck and Wassmann, 1996; Reigstad and Wassmann, 1996; Reigstad et al., 2000), Fanafjorden (western Norway, Wassmann, 1984) and Conception Bay (Canada, Thompson et al., 2008; Table 4), but were comparable with fluxes found in the open Barents Sea (Olli et al., 2002; Table 4). We argue for a two-fold explanation of the decline in vertical biomass flux during the course of the spring bloom (Fig. 4). First, the intensifying top-down regulation by zooplankton probably reduced the vertical flux from Spring I to III (Fig. 4). Second, the observed shift in the phytoplankton bloom composition from diatom-dominated during Spring I to *Phaeocystis*-dominated during Spring III (Kubiszyn et al., in prep.) could impact the vertical flux. Diatoms are known to produce sticky exopolymeric substances, which promote aggregate formation and sinking (Kiørboe et al., 1990; Smetacek, 1985; Thornton, 2002). Because diatoms were also abundant in the sediment traps during Spring I (molecular 454-sequencing analysis, M. Marquardt, pers. com.), we suggest that they contributed to the higher vertical flux rates during early spring. The small celled flagellate *Phaeocystis pouchetii* dominated in the water column during Spring III (> 10^6 cells L^{-1}, Kubiszyn et al., in prep.) and *Phaeocystis pouchetii* was also identified in the IsA sediment traps down to 60 m (454-sequencing, M. Marquardt, pers. com.). However, literature indicates that this species contributes little to the vertical carbon flux at depth > 60 m, despite high suspended concentrations (Reigstad and Wassmann, 2007; Reigstad et al., 2000).

Our estimated bulk sinking velocities (Table 2) further pinpointed a slowing down of the vertical flux during the course of the bloom. This matches the argumentation on a shift from fast-sinking diatoms (Passow, 1991) to slow-sinking detritus, including *Phaeocystis* cells (Reigstad and Wassmann, 2007).

The interpretation of Autumn I data was complex. Glacial run-off occurs in Adventfjorden between June and September when air temperatures (> 0° C) allow snow and glacial melting on land (Węsławski et al., 1999). The tide- and wind-steered meandering glacial plume affected IsA at the surface (seen as reduced surface salinity in Fig. 2, Fig. A.1), but other impacting effects must also be assumed at depths. Our POC flux during Autumn I exceeded reported literature values up to 30-fold (Table 4) and was also higher than the flux observed during Spring I-III (Fig. 4). We suggest that this was linked to the glacial run-off.

Zajaczkowski et al. (2010) described an intense vertical flux of particulate inorganic and organic material (PIM and POM, respectively) in Adventfjorden during the summer melting period. Accordingly, we assume that entrained POM also enhanced the POC flux at IsA. This is bolstered by a high C/N ratio (up to 16, suggesting degraded re-suspended or terrestrial material) in the sinking material in both the present study (Table 3) and Zajączkowski et al. (2010).

Glacial melt water can form "fingers" of high concentration of suspended particulate matter, stretching several kilometers from the Advent River inlet into the fjord (Zajączkowski and Włodarska-Kowalczuk, 2007). We assume that this possibly promoted physical flocculation, a process in which unstable mineral particles, suspended in the entrained melt water, form aggregates with high sinking velocity (Kranck, 1973; Sutherland et al., 2015; Syvitski, 1980). The lithogenic material was probably also incooperated into aggregates and fecal pellets, and ballasted organic biomass due to its high specific sinking velocity (Iversen et al., 2010; Ploug et al., 2008) and increased the vertical POC flux.

The comparison with literature shows that the vertical Chl *a* and POC flux at IsA was congruent with the previously reported fluxes in other ice-free high latitude systems during winter and spring but was higher during autumn.

4.3 Sinking particles' characteristics during different seasons

Drivers of physical and biological particle aggregation (e.g., shear, cell abundance, stickiness, Kiørboe et al., 1994) and modification processes by grazers (Turner, 2002; Turner, 2015) affect sinking particles' characteristics, such as C/N ratio, size, and sinking velocity (De La

Rocha and Passow, 2007). Here, we discuss the characteristics of the sinking material at IsA during the different seasons and possible drivers.

In our study, the C/N ratio of sinking material matched well with the visual analysis (Table 3). Both implied the sedimentation of degenerated material in mid-December (Winter I) and recently produced material during mid-May and late May (Spring II and III, respectively, Table 3). A high C/N ratio, as found during Autumn I (Table 3), usually points toward strongly degraded material or terrestrial material, but the visual inspection (20 m and 30 m gels) suggested sinking of aggregates and fecal pellets (Table 3). We presume that the impact of the meandering glacial plume on IsA was highly variable. When the track of the plume covered IsA, the sinking material had a higher C/N ratio due to more terrestrial material when compared to a situation when the plume followed an alternative route, not hitting IsA. This explanation is supported by the high C/N ratios of the 24 h deployed traps (13.0-15.0, Table 3), but lower ones in the subsequently deployed 2 h gel traps (C/N ratio 6.5-8.8, fresh material observed on the gels, data not shown), as well as the high variability of salinity and density (Fig. A.1).

The average sinking velocity for total POC or Chl *a* biomass (Table 2) at IsA during winter and spring was comparable with the average velocities reported by Kiørboe et al. (1994) in the Danish Isefjorden (10 m), but was somewhat higher than rates at Nordvestbanken (off the Norwegian Shelf, 100 m, Andreassen et al., 1999). A direct comparison with particle sinking velocities estimated by Laurenceau-Cornec et al. (2015) or McDonnell and Buesseler (2010) was difficult, because the calculations were based on different data (our study: integrated biomass and biomass flux; other studies: particle abundance in water column and sediment traps) and differed in the size fraction included in the study (our study: > 0.7 µm, Laurenceau-Cornec et al, 2015: > 150 µm, McDonnell and Buesseler, 2010: > 50 µm).

Following Stokes' Law, which tightly couples particle size and sinking velocity, the highest sinking rates in our study were expected at 60 m, where particles tended to be larger than at shallower depths. Our estimates of the sinking velocity at 30 m and 60 m support this anticipation (Table 2).

In addition, Stokes' Law would suggest higher sinking velocities during Winter I and Autumn I (40, 60 m), where particles tended to be larger than during Spring II, III and Autumn I (20, 30 m, Fig. 5). In case of Autumn I (40, 60 m) the suggestion of Stokes' Law is supported (Table 2): We found here large particles and a high sinking velocity. Particle sizes in the 20 m and 30 m gels during Autumn I however pinpointed that sinking velocity is not merely influenced by size, but a variety of parameters such as sinking particle type, density, and

mineral ballasting (De La Rocha and Passow, 2007; Iversen et al., 2010; Laurenceau-Cornec et al., 2015; McDonnell and Buesseler, 2010). We suggest that incooperation of lithogenic material into organic particles (Iversen et al., 2010) and a higher abundance of fast-sinking fecal pellets (Table 3) overruled the size effect at the shallow sampling depth during Autumn I, and caused the high sinking velocity. During Winter I, the low sinking velocity was apparently a result of prevailing large, fluffy, detrital particles (Table 3) with a low specific weight and the lack of ballasting diatoms (Iversen and Ploug, 2010) or lithogenic material (no run-off during winter).

Precautions must thus be taken when relating particle size or volume to the POC flux. For Winter I we calculated a low POC: volume ratio of ~0.0003 mg POC mm^{-3} (data not shown), which reflects the high contribution of fluffy detritus. The ratios from Spring II were among the highest during the present study (e.g., 30 m: 0.0050 mg POC mm^{-3}) and reflected the higher contribution of aggregates and fecal pellets. However, all POC: volume ratios at IsA were several magnitudes lower when compared to ratios from the central Barents Sea, where sinking material comprised densely packed unidentifiable detritus and fecal material (0.0067-0.1101 mg POC mm^{-3}, Wiedmann et al., 2014). Accordingly, translating particle size or volume into POC flux without considering the prevailing particle type may introduce large errors.

Pteropod sedimentation events were observed during autumn and winter in the North Atlantic, and were also found at IsA (Table 3). The reported abundances range from 24 individuals m^{-2} d^{-1} at 1700-2800 m in the Fram Strait (Meinecke and Wefer, 1990) to ca. $18*10^3$ individuals m^{-2} d^{-1} at 50 m in the Norwegian Sea (Bathmann et al., 1991) and are comparable with our observations at IsA (~$8*10^3$ m^{-2} d^{-1}, Table 3). High pteropod abundances may have enhanced the POC flux during Autumn I, but because our gel trap data did not indicate if these pelagic gastropods were actively swimming or passively sinking into the trap cylinders, we cannot state if the animals also represented a true component of the vertical biomass flux. Nevertheless, they seem to provide an important mechanism for vertical export, because lost or rejected mucous feeding webs of pteropds can promote aggregate formation (Bathmann et al., 1991; Noji et al., 1997) and enhance the sinking velocity of organic matter.

4.4 Ecosystem functioning during different seasons in high Arctic ice-free fjord with a major glacial run-off during autumn

In the context of climate warming, it is likely that seasonally ice-covered Arctic fjords and embayments may become permanently ice-free in the future. To predict the vertical flux

intensity in these areas, an improved understanding is needed. We used Adventfjorden as a model area, because it has been seasonally ice-covered for several months during 2000-2005 (www.met.no, detailed ice maps available for Adventfjorden since 2000), but tended to be ice-free during the last years (2006-2007, 2010, 2012-2014). This was probably a result of strong northerly winds, which enhanced the advection of comparably warm water from the West Spitsbergen Current into the fjords on western Svalbard (Cottier et al., 2007) and higher temperature of the advected water (Onarheim et al., 2014).

Compiling our data, we put forward a conceptual model of the pelagic-benthic coupling in a year-round ice-free Arctic fjord with glacial run-off during autumn (Fig. 7). In terms of suspended POC and Chl *a* concentrations as well as the vertical biomass flux, the winter situation in Adventfjorden was comparable to boreal, sub-Arctic and ice-free Arctic fjords. Enhanced mixing by thermal convection and wind must be assumed when compared to the previous ice-covered situation. We presume that detrital material, previously settled to the bottom, was re-suspended, especially in the shallow areas, and laterally advected to the middle of the fjord as described for the sub-Arctic Ramfjorden (Noji et al., 1993). The vertical flux during the polar night was dominated by large detrital particles with a low density and POC content. In the absence of ballasting materials (e.g., diatom cells or lithogenic material), the sinking velocity and POC flux tended to be lower when compared to the other seasons (Table 2, Fig. 4, Fig. 7).

The spring situation at IsA resembled previous observation from boreal, sub-Arctic and Arctic ice-free fjords in terms of suspended and sedimenting Chl *a* and POC. High vertical flux rates of un-grazed phytoplankton aggregates and detrital material was found during an early bloom phase, but the vertical flux intensity decreased toward the late bloom. We suggest this was caused by a shift from a diatom to a *Phaeocystis* dominated bloom as well as an intensifying top-down control by zooplankton.

During autumn, the ice-free Adventfjorden differed from many investigated fjords e.g., in northern Norway (Table 4), which are rarely affected by major glacial run-off (Fig. 2). We did not observe any phytoplankton autumn blooms and associated POC sedimentation events as described for sub-Arctic regions (Wassmann et al., 1991), but this may be due to low sampling frequency. Instead, the sediment loaded meltwater input was identified as a major driver of the high POC flux during autumn. In addition, high abundances of *Limacina* sp. and rejected or lost mucous nets may be possible drivers of the high POC flux.

We propose that the seasonal vertical flux patterns in an ice-free Arctic fjord with glacial run-off resemble sub-Arctic fjords during winter and spring. During autumn, the systems appear to differ and a major POC sedimentation may be caused by the glacial run-off.

In a scenario of climate warming it must be assumed that previously ice-covered fjords and embayments will turn into permanently open waters in the future. Ice algae blooms associated with the sea ice and their contribution to the vertical carbon flux will no longer occur in these future ice-free fjords. Fjords, affected by glacial run-off, may however still have a high vertical biomass flux because the entrained sediment-loaded melt water can drive the vertical biomass flux in the fjord during the melting season.

Acknowledgements

We would like to thank the captain and the crew of the NorCGV Svalbard, the R/V Helmer Hanssen, R/V Viking and the M/S Farm for great assistance during sampling under the sometimes harsh condition. A helping hand was highly appreciated in the field (E. I. Stübner), during the CHN analyses (S. Øygaarden), and with the hydrographical data (R. Skogseth). We also thank A. M. Kubiszyn and E. I. Stübner for insight in their plankton data and two anonymous reviewers for their comments, which improved this work substantially. The field work was partly funded by the Arctic Field Grant (RIS 5264) and the CONFLUX project (Tromsø Forskningsstiftelse).

Literature

Alldredge, A.L., Silver, M.W., 1988. Characteristics, dynamics and significance of marine snow. Prog. Oceanogr. 20, 41-82. doi: 10.1016/0079-6611(88)90053-5.

Andreassen, I.J., Wassman, P., Ratkova, T.N., 1999. Seasonal variation of vertical flux of phytyoplankton and biogenic matter at Nordvestbanken, north Norwegian shelf in 1994. Sarsia 84, 227-238.

Arendt, K.E., Juul-Pedersen, T., Mortensen, J., Blicher, M.E., Rysgaard, S., 2013. A 5-year study of seasonal patterns in mesozooplankton community structure in a sub-Arctic fjord reveals dominance of *Microsetella norvegica* (Crustacea, Copepoda). J. Plankton Res. 35, 105-120. doi: 10.1093/plankt/fbs087.

Arrigo, K.R., 2014. Sea Ice Ecosystems. Annu. Rev. Mar. Sci. 6, 439-467. doi: 10.1146/annurev-marine-010213-135103.

Bathmann, U.V., Noji, T.T., von Bodungen, B., 1991. Sedimentation of pteropods in the Norwegian Sea in autumn. Deep-Sea Res. I 38, 1341-1360. doi: 10.1016/0198-0149(91)90031-A.

Bianchi, T.S., 2006. Biochemistry of Estuaries. Oxford University Press, Cary, USA 720 pp.

569 Calbet, A., Riisgaard, K., Saiz, E., Zamora, S., Stedmon, C., Nielsen, T.G., 2011. Phytoplankton
570 growth and microzooplankton grazing along a sub-Arctic fjord (Godthåbsfjord, west
571 Greenland). Mar. Ecol. Prog. Ser. 442, 11-22. doi: 10.3354/meps09343.
572 Cottier, F.R., Nilsen, F., Inall, M.E., Gerland, S., Tverberg, V., Svendsen, H., 2007. Wintertime
573 warming of an Arctic shelf in response to large-scale atmospheric circulation. Geophys. Res.
574 Lett. 34, L10607. doi: 10.1029/2007GL029948.
575 De La Rocha, C.L., Passow, U., 2007. Factors influencing the sinking of POC and the efficiency of the
576 biological carbon pump. Deep-Sea Res. II 54, 639-658. doi: 10.1016/j.dsr2.2007.01.004.
577 Degerlund, M., Eilertsen, H.C., 2010. Main Species Characteristics of Phytoplankton Spring Blooms
578 in NE Atlantic and Arctic Waters (68-80° N). Estuar. Coasts 33, 242-269. doi:
579 10.1007/s12237-009-9167-7.
580 Ebersbach, F., Trull, T.W., 2008. Sinking particle properties from polyacrylamide gels during the
581 Kerguelen Ocean and Plateau compared Study (KEOPS): Zooplankton control of carbon
582 export in an area of persistent natural iron inputs in the Southern Ocean. Limnol. Oceanogr.
583 53, 212-224. doi: 10.2307/40006162.
584 Eilertsen, H.C., 1993. Spring blooms and stratification. Nature 363, 24-24. doi: 10.1038/363024a0.
585 Eilertsen, H.C., Degerlund, M., 2010. Phytoplankton and light during the northern high-latitude
586 winter. J. Plankton Res. 32, 899-912. doi: 10.1093/plankt/fbq017.
587 Eilertsen, H.C., Frantzen, S., 2007. Phytoplankton from two sub-Arctic fjords in northern Norway
588 2002–2004: I. Seasonal variations in chlorophyll a and bloom dynamics. Mar. Biol. Res. 3,
589 319-332. doi: 10.1080/17451000701632877.
590 Eilertsen, H.C., Schei, B., Taasen, J.P., 1981. Investigations on the plankton community of
591 Balsfjorden, Northern Norway. The phytoplankton 1976 - 1978. Abundance, species
592 composition, and succession. Sarsia 66, 129-141.
593 Forest, A., Babin, M., Stemmann, L., Picheral, M., Sampei, M., Fortier, L., Gratton, Y., Bélanger, S.,
594 Devred, E., Sahlin, J., Doxaran, D., Joux, F., Ortega-Retuerta, E., Martín, J., Jeffrey, W.H.,
595 Gasser, B., Carlos Miquel, J., 2013. Ecosystem function and particle flux dynamics across the
596 Mackenzie Shelf (Beaufort Sea, Arctic Ocean): an integrative analysis of spatial variability
597 and biophysical forcings. Biogeosciences 10, 2833-2866. doi: 10.5194/bg-10-2833-2013.
598 Iversen, K.R., Seuthe, L., 2011. Seasonal microbial processes in a high-latitude fjord (Kongsfjorden,
599 Svalbard): I. Heterotrophic bacteria, picoplankton and nanoflagellates. Polar Biol. 34, 731-
600 749. doi: 10.1007/s00300-010-0929-2.
601 Iversen, M.H., Nowald, N., Ploug, H., Jackson, G.A., Fischer, G., 2010. High resolution profiles of
602 vertical particulate organic matter export off Cape Blanc, Mauritania: Degradation processes
603 and ballasting effects. Deep-Sea Res. I 57, 771-784. doi:
604 dx.doi.org/10.1016/j.dsr.2010.03.007.
605 Iversen, M.H., Ploug, H., 2010. Ballast minerals and the sinking carbon flux in the ocean: carbon-
606 specific respiration rates and sinking velocity of marine snow aggregates. Biogeosciences 7,
607 2613-2624. doi: 10.5194/bg-7-2613-2010.
608 Jackson, G.A., Maffione, R., Costello, D.K., Alldredge, A.L., Logan, B.E., Dam, H.G., 1997. Particle
609 size spectra between 1 μm and 1 cm at Monterey Bay determined using multiple instruments.
610 Deep-Sea Res. I 44, 1739-1767. doi: 10.1016/S0967-0637(97)00029-0.
611 Jackson, G.A., Waite, A.M., Boyd, P.W., 2005. Role of algal aggregation in vertical carbon export
612 during SOIREE and in other low biomass environments. Geophys. Res. Lett. 32, L13607. doi:
613 10.1029/2005gl023180.
614 Ji, R., Jin, M., Varpe, Ø., 2013. Sea ice phenology and timing of primary production pulses in the
615 Arctic Ocean. Glob. Change Biol. 19, 734-741. doi: 10.1111/gcb.12074.
616 Keck, A., Wassmann, P., 1996. Temporal and spatial patterns of sedimentation in the subarctic fjord
617 Malangen, Northern Norway. Sarsia 80, 259-276.
618 Kiørboe, T., Andersen, K.P., Dam, H.G., 1990. Coagulation efficiency and aggregate formation in
619 marine phytoplankton. Mar. Biol. 107, 235-245. doi: 10.1007/BF01319822.
620 Kiørboe, T., Lundsgaard, C., Olesen, M., Hansen, J.L.S., 1994. Aggregation and sedimentation
621 processes during a spring phytoplankton bloom: A field experiment to test coagulation theory.
622 J. Mar. Res. 52, 297-323. doi: 10.1357/0022240943077145.

623 Kranck, K., 1973. Flocculation of Suspended Sediment in the Sea. Nature 246, 348-350. doi:
624 10.1038/246348a0.
625 Kubiszyn, A.M., Wiktor, J.M., Wiktor, J.M.J., Griffiths, C., Kristiansen, S., T.M., G., The annual
626 planktonic protist community structure in an ice-free high Arctic fjord (Adventfjorden, West
627 Spitsbergen). Prepared for submission to J. Plankton Res.
628 Lampitt, R.S., 2001. Marine Snow, in: Steele, J.H., Thorpe, S.A., Turekian, K.K. (Eds.), Encyclopedia
629 of Ocean Sciences. Academic Press, San Diego, USA, pp. 1667-1675. doi:
630 10.1006/rwos.2001.0218.
631 Laurenceau-Cornec, E.C., Trull, T.W., Davies, D.M., De La Rocha, C.L., Blain, S., 2015.
632 Phytoplankton morphology controls on marine snow sinking velocity. Mar. Ecol. Prog. Ser.
633 520, 35-56. doi: 10.3354/meps11116.
634 Leu, E., Søreide, J.E., Hessen, D.O., Falk-Petersen, S., Berge, J., 2011. Consequences of changing sea-
635 ice cover for primary and secondary producers in the European Arctic shelf seas: Timing,
636 quantity, and quality. Progr. Oceanogr. 90, 18-32. doi: 10.1016/j.pocean.2011.02.004.
637 Lundsgaard, C., M., O., Reigstad, M., Olli, K., 1999. Sources of settling material: aggregation and
638 zooplankton mediated fluxes in the Gulf of Riga. J. Mar. Syst. 23, 197–210. doi:
639 10.1016/S0924-7963(99)00058-5.
640 Mantoura, R.F.C., Wright, S.W., Barlow, R.G., Cummings, D.E., 1997. Filtration and storage of
641 pigments from microalgae. Monographs on Oceanographic Methodology, in: Jeffrey, S.W.,
642 Mantoura, R.F.C., Wright, S.W. (Eds.), Phytoplankton pigments in oceanography: guidelines
643 to modern methods. UNESCO Publishing, Paris.
644 McDonnell, A.M.P., Buesseler, K.O., 2010. Variability in the average sinking velocity of marine
645 particles. Limnol. Oceanogr. 55, 2085-2096. doi: 10.4319/lo.2010.55.5.2085.
646 Meinecke, G., Wefer, G., 1990. Seasonal pteropod sedimentation in the Norwegian Sea. Palaeogeogr.
647 Palaeocl. 79, 129-147. doi: 10.1016/0031-0182(90)90109-K.
648 Noji, T.T., Bathmann, U.V., Bodungen, B.v., Voss, M., Antia, A., Krumbholz, M., Klein, B., Peeken,
649 I., Noji, C.I.-M., Rey, F., 1997. Clearance of picoplankton-sized particles and formation of
650 rapidly sinking aggregates by the pteropod, *Limacina retroversa*. J. Plankton Res. 19, 863-
651 875. doi: 10.1093/plankt/19.7.863.
652 Noji, T.T., Estep, K.W., Macintyre, F., Norrbin, F., 1991. Image analysis of faecal material grazed
653 upon by three species of copepods: evidence for coprorhexy, coprophagy and coprochaly. J.
654 Mar. Biol. Assoc. UK 71, 465-480. doi: 10.1017/S0025315400051717.
655 Noji, T.T., Noji, C.I.-M., Barthel, K.-G., 1993. Pelagic-benthic coupling during the onset of winter in
656 a northern Norwegian fjord. Carbon flow and fate of suspended particulate matter. Mar. Ecol.
657 Prog. Ser. 93, 89-99.
658 Olli, K., Rieser, C.W., Wassmann, P., Ratkova, T., Arashkevich, E., Pasternak, A., 2002. Seasonal
659 variation in vertical flux of biogenic matter in the marginal ice zone and the central Barents
660 Sea. J. Mar. Syst. 38, 189-204. doi: 10.1016/S0924-7963(02)00177-X
661 Onarheim, I.H., Smedsrud, L.H., Ingvaldsen, R.B., Nilsen, F., 2014. Loss of sea ice during winter
662 north of Svalbard. Tellus A 66, 23933. doi: 10.3402/tellusa.v66.23933.
663 Otsu, N., 1979. A Threshold Selection Method from Gray-Level Histograms. IEEE T. Syst. Man Cyb.
664 9, 62-66. doi: 10.1109/TSMC.1979.4310076.
665 Parsons, T.R., Lalli, C.M., 1988. Comparative oceanic ecology of the plankton communities of
666 subarctic Atlantic and Pacific Oceans. Oceanogr. Mar. Biol. Annu. Rev. 26, 317-359.
667 Passow, U., 1991. Species-specific sedimentation and sinking velocities of diatoms. Mar. Biol. 108,
668 449-455. doi: 10.1007/BF01313655.
669 Passow, U., De La Rocha, C.L., 2006. Accumulation of mineral ballast on organic aggregates. Global
670 Biogeochem. Cy. 20, GB1013. doi: 10.1029/2005GB002579.
671 Peinert, R., von Bodungen, B., Smetacek, V.S., 1989. Food Web Structure and Loss Rate, in: Berger,
672 W.H., Smetacek, V.S., Wefer, G. (Eds.), Productivity of the ocean: present and past. Wiley,
673 Berlin, pp. 35-48.
674 Ploug, H., Iversen, M.H., Fischer, G., 2008. Ballast, sinking velocity, and apparent diffusivity within
675 marine snow and zooplankton fecal pellets: Implications for substrate turnover by attached
676 bacteria. Limnol. Oceanogr. 53, 1878-1886. doi: 10.4319/lo.2008.53.5.1878.

677 Rat'kova, T.N., Wassmann, P., 2002. Seasonal variation and spatial distribution of phyto- and
678 protozooplankton in the central Barents Sea. J. Mar. Syst. 38, 47-75. doi: 10.1016/s0924-
679 7963(02)00169-0.
680 Reigstad, M., Riser, C.W., Wassmann, P., Ratkova, T., 2008. Vertical export of particulate organic
681 carbon: Attenuation, composition and loss rates in the northern Barents Sea. Deep-Sea Res. II
682 55, 2308-2319. doi: 10.1016/j.dsr2.2008.05.007.
683 Reigstad, M., Wassmann, P., 1996. Importance of advection for pelagic-benthic coupling in north
684 Norwegian fjords. Sarsia 80, 245-257. doi: 10.1080/00364827.1996.10413599.
685 Reigstad, M., Wassmann, P., 2007. Does *Phaeocystis* spp. contribute significantly to vertical export of
686 organic carbon? Biogeochemistry 83, 217-234. doi: 10.1007/s10533-007-9093-3.
687 Reigstad, M., Wassmann, P., Ratkova, T., Arashkevich, E., Pasternak, A., Øygarden, S., 2000.
688 Comparison of the springtime vertical export of biogenic matter in three northern Norwegian
689 fjords. Mar. Ecol. Prog. Ser. 201, 73-80. doi: 10.3354/meps201073.
690 Rynearson, T.A., Richardson, K., Lampitt, R.S., Sieracki, M.E., Poulton, A.J., Lyngsgaard, M.M.,
691 Perry, M.J., 2013. Major contribution of diatom resting spores to vertical flux in the sub-polar
692 North Atlantic. Deep-Sea Res. I 82, 60-71. doi: 10.1016/j.dsr.2013.07.013.
693 Smayda, T.J., 1971. Normal and accelerated sinking of phytoplankton in the sea. Mar. Geol. 11, 105-
694 122. doi: 10.1016/0025-3227(71)90070-3.
695 Smetacek, V.S., 1985. Role of Sinking in Diatom Life-History Cycles - Ecological, Evolutionary and
696 Geological Significance. Mar. Biol. 84, 239-251. doi: 10.1007/bf00392493.
697 Smith, R.W., Bianchi, T.S., Allison, M., Savage, C., Galy, V., 2015. High rates of organic carbon
698 burial in fjord sediments globally. Nat. Geosci. 8, 450-453. doi: 10.1038/ngeo2421.
699 Stübner, E.I., Søreide, J.E., Reigstad, M., Marquardt, M., Blachowiak-Samolyk, K., Common
700 strangers – seasonal meroplankton dynamics at high latitudes in Adventfjorden, Svalbard.
701 Submitted to J. Plankton Res.
702 Sutherland, B.R., Barrett, K.J., Gingras, M.K., 2015. Clay settling in fresh and salt water. Environ.
703 Fluid. Mech. 15, 147-160. doi: 10.1007/s10652-014-9365-0.
704 Svensen, C., Wexels Riser, C., Reigstad, M., Seuthe, L., 2012. Degradation of copepod faecal pellets
705 in the upper layer: role of microbial community and *Calanus finmarchicus*. Mar. Ecol. Prog.
706 Ser. 462, 39-49. doi: 10.3354/meps09808.
707 Syvitski, J.M., 1980. Flocculation, Agglomeration, and Zooplankton Pelletization of Suspended
708 Sediment in a Fjord Receiving Glacial Meltwater, in: Freeland, H., Farmer, D., Levings, C.
709 (Eds.), Fjord Oceanography. Springer US, pp. 615-623.
710 Søreide, J.E., Leu, E., Berge, J., Graeve, M., Falk-Petersen, S., 2010. Timing of blooms, algal food
711 quality and *Calanus glacialis* reproduction and growth in a changing Arctic. Glob. Change
712 Biol. 16, 3154-3163. doi: 10.1111/j.1365-2486.2010.02175.x.
713 Thiele, S., Fuchs, B.M., Amann, R., Iversen, M.H., 2015. Colonization in the photic zone and
714 subsequent changes during sinking determines bacterial community composition in marine
715 snow. Appl. Environ. Microbiol. 81, 1463-1471. doi: 10.1128/aem.02570-14.
716 Thompson, R.J., Deibel, D., Redden, A.M., McKenzie, C.H., 2008. Vertical flux and fate of
717 particulate matter in a Newfoundland fjord at sub-zero water temperatures during spring. Mar.
718 Ecol. Prog. Ser. 357, 33-49. doi: 10.3354/meps07277.
719 Thornton, D., 2002. Diatom aggregation in the sea: mechanisms and ecological implications. Eur. J.
720 Phycol. 37, 149-161. doi: 10.1017/S0967026202003657.
721 Tommasi, D., Hunt, B.P.V., Pakhomov, E.A., Mackas, D.L., 2013. Mesozooplankton community
722 seasonal succession and its drivers: Insights from a British Columbia, Canada, fjord. J Mar.
723 Sys. 115–116, 10-32. doi: 10.1016/j.jmarsys.2013.01.005.
724 Townsend, D.W., Keller, M.D., Sieracki, M.E., Ackleson, S.G., 1992. Spring phytoplankton blooms in
725 the absence of vertical water column stratification. Nature 360, 59-62. doi: 10.1038/360059a0.
726 Tremblay, C., Runge, J., Legendre, L., 1989. Grazing and sedimentation of ice algae during and
727 immediately after a bloom at the ice-water interface. Mar. Ecol. Prog. Ser. 56, 291-300.
728 Tremblay, J.-É., Gagnon, J., 2009. The effects of irradiance and nutrient supply on the productivity of
729 Arctic waters: a perspective on climate change, in: Nihoul, J.C.J., Kostianoy, A.G. (Eds.),
730 Influence of Climate Change on the Changing Arctic and Sub-Arctic Conditions. Springer
731 Netherlands, pp. 73-93.

Turner, J.T., 2002. Zooplankton fecal pellets, marine snow and sinking phytoplankton blooms. Aquat. Microb. Ecol. 27, 57-102. doi: 10.3354/ame027057.
Turner, J.T., 2015. Zooplankton fecal pellets, marine snow, phytodetritus and the ocean's biological pump. Prog. Oceanogr. 130, 205-248. doi: 10.1016/j.pocean.2014.08.005.
Wassmann, P., 1984. Sedimentation and benthic mineralization of organic detritus in a Norwegian fjord. Mar. Biol. 83, 83-94. doi: 10.1007/BF00393088.
Wassmann, P., Peinert, R., Smetacek, V., 1991. Patterns of production and sedimentation in the boreal and polar Northeast Atlantic. Proceedings of the Pro Mare Symposium on Polar Marine Ecology, Trondheim, 12-16 May 1990. Pol. Res. 10, 209-228. doi: 10.1111/j.1751-8369.1991.tb00647.x.
Wassmann, P., Svendsen, H., Keck, A., Reigstad, M., 1996. Selected aspects of the physical oceanography and particle fluxes in fjords of northern Norway. J. Mar. Syst. 8, 53-71.
Węsławski, J.M., Kwasniewski, S., Wiktor, J., 1991. Winter in a Svalbard fjord ecosystem. Arctic 44, 115-123. doi: 10.14430/arctic1527115-123.
Węsławski, J.M., Szymelfenig, M., Zajączkowski, M., Keck, A., 1999. Influence of salinity and suspended matter of benthos of an Arctic tidal flat. ICES J. Mar. Sci. 56 Supplement, 194-202.
Wexels Riser, C., Wassmann, P., Reigstad, M., Seuthe, L., 2008. Vertical flux regulation by zooplankton in the northern Barents Sea during Arctic spring. Deep Sea Research Part II: Topical Studies in Oceanography 55, 2320-2329. doi: 10.1016/j.dsr2.2008.05.006.
Weydmann, A., Søreide, J.E., Kwaśniewski, S., Leu, E., Falk-Petersen, S., Berge, J., 2013. Ice-related seasonality in zooplankton community composition in a high Arctic fjord. J. Plankton Res. 35, 831-842. doi: 10.1093/plankt/fbt031.
Wiedmann, I., Reigstad, M., Sundfjord, A., Basedow, S., 2014. Potential drivers of sinking particle's size spectra and vertical flux of particulate organic carbon (POC): Turbulence, phytoplankton, and zooplankton. J. Geophys. Res.-Oceans 119, 6900-6917. doi: 10.1002/2013JC009754.
Zajączkowski, M., Nygård, H., Hegseth, E.N., Berge, J., 2010. Vertical flux of particulate matter in an Arctic fjord: the case of lack of the sea-ice cover in Adventfjorden 2006-2007. Polar Biol. 33, 223-239. doi: 10.1007/s00300-009-0699-x.
Zajączkowski, M., Włodarska-Kowalczuk, M., 2007. Dynamic sedimentary environments of an Arctic glacier-fed river estuary (Adventfjorden, Svalbard). I. Flux, deposition, and sediment dynamics. Estuar. Coastal Shelf S. 74, 285-296. doi: 10.1016/j.ecss.2007.04.015.

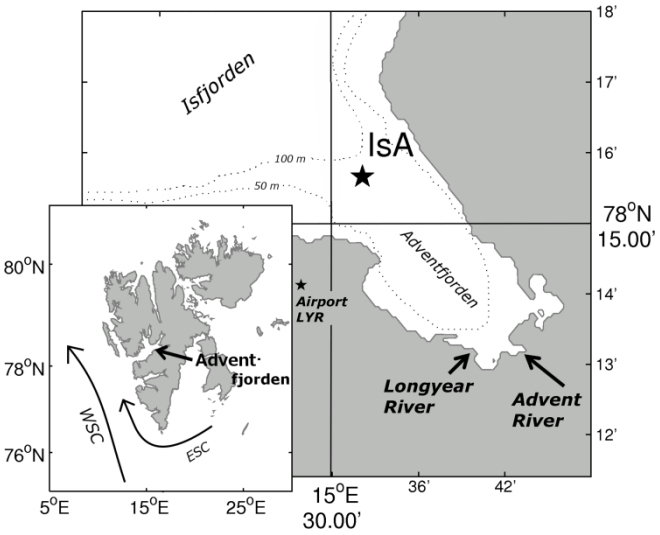

Figure 1: IsA station was located in the mouth of Adventfjorden, a side branch of the Isfjorden system, western Svalbard (main map, depth contour following Zajączkowski et al., 2010). Adventfjorden is influenced by the Atlantic derived, warm West Spitsbergen Current (WSC) and the Arctic derived, cold East Spitsbergen Current (ESC, small map), as well as glacial run-off from the Longyear and Advent River (during ice melting period in summer and autumn).

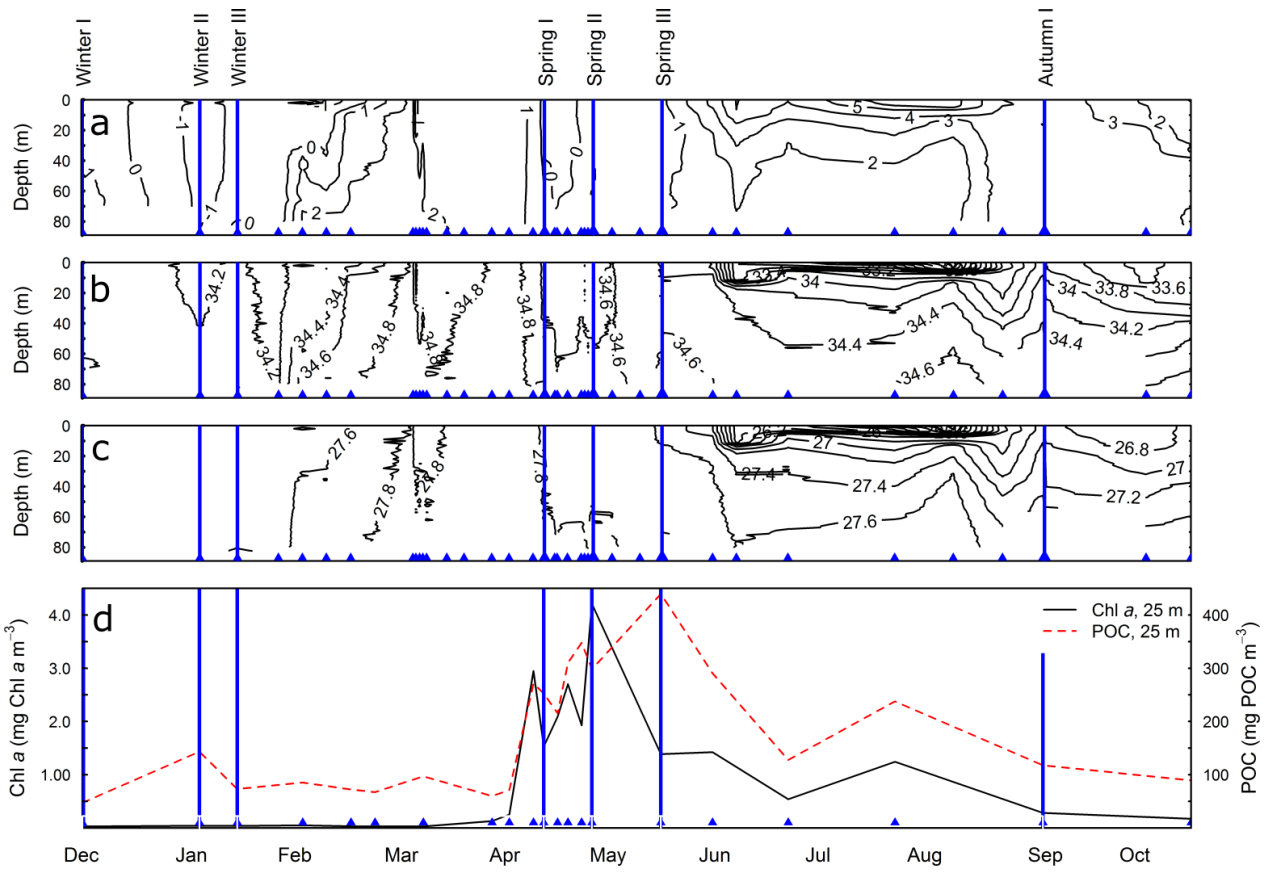

Figure 2: Temperature (a), salinity (b), density (c), and the seasonal development of suspended biomass is shown (d, black line: chlorophyll *a*, Chl *a*, red stippled line: particulate organic carbon, POC) at IsA during the sampling program (14.12.2011 - 31.10.2012). Sampling dates with the CTD are indicated by blue triangles. Sediment trap deployment took place at the dates indicated by blue vertical lines.

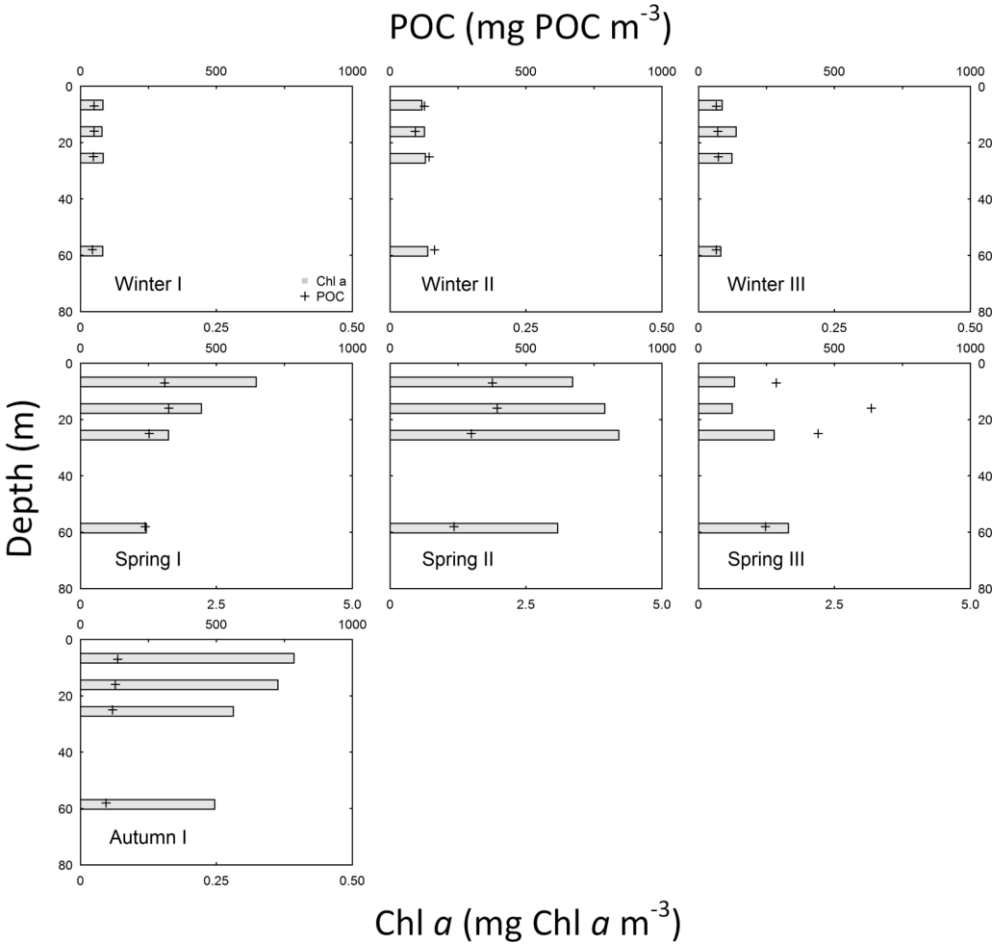

Figure 3: Suspended chlorophyll *a* (Chl *a*) (grey bars) and particulate organic carbon (POC, black cross) concentrations at 5, 15, 25 and 60 m during Winter I-III, Spring I-III and Autumn I. Note different scales on the lower x-axis for Spring I-III.

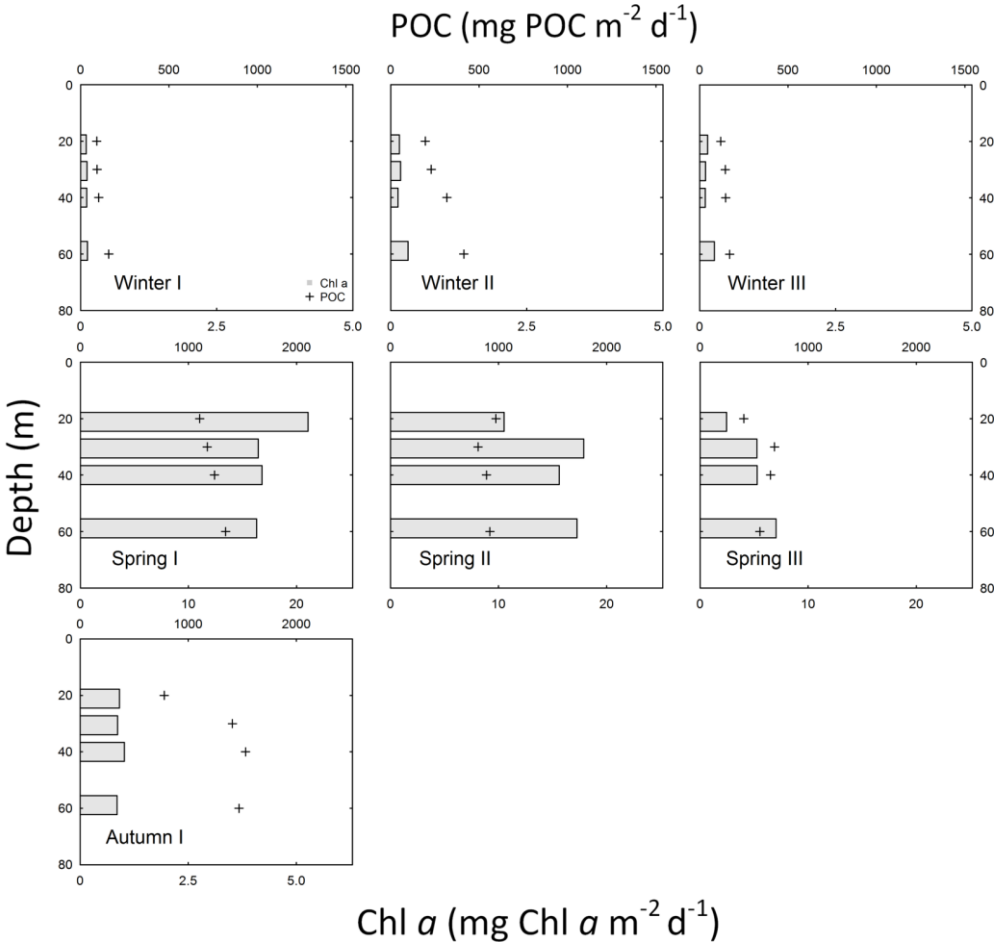

Figure 4: Vertical flux of chlorophyll *a* (Chl *a*, grey bars) and particulate organic carbon (POC, black cross) at 20, 30, 40, and 60 m during Winter I-III , Spring I-III, and Autumn I. Note different scale on the upper x-axis during Winter I-III and the lower x-axis for Spring I-III.

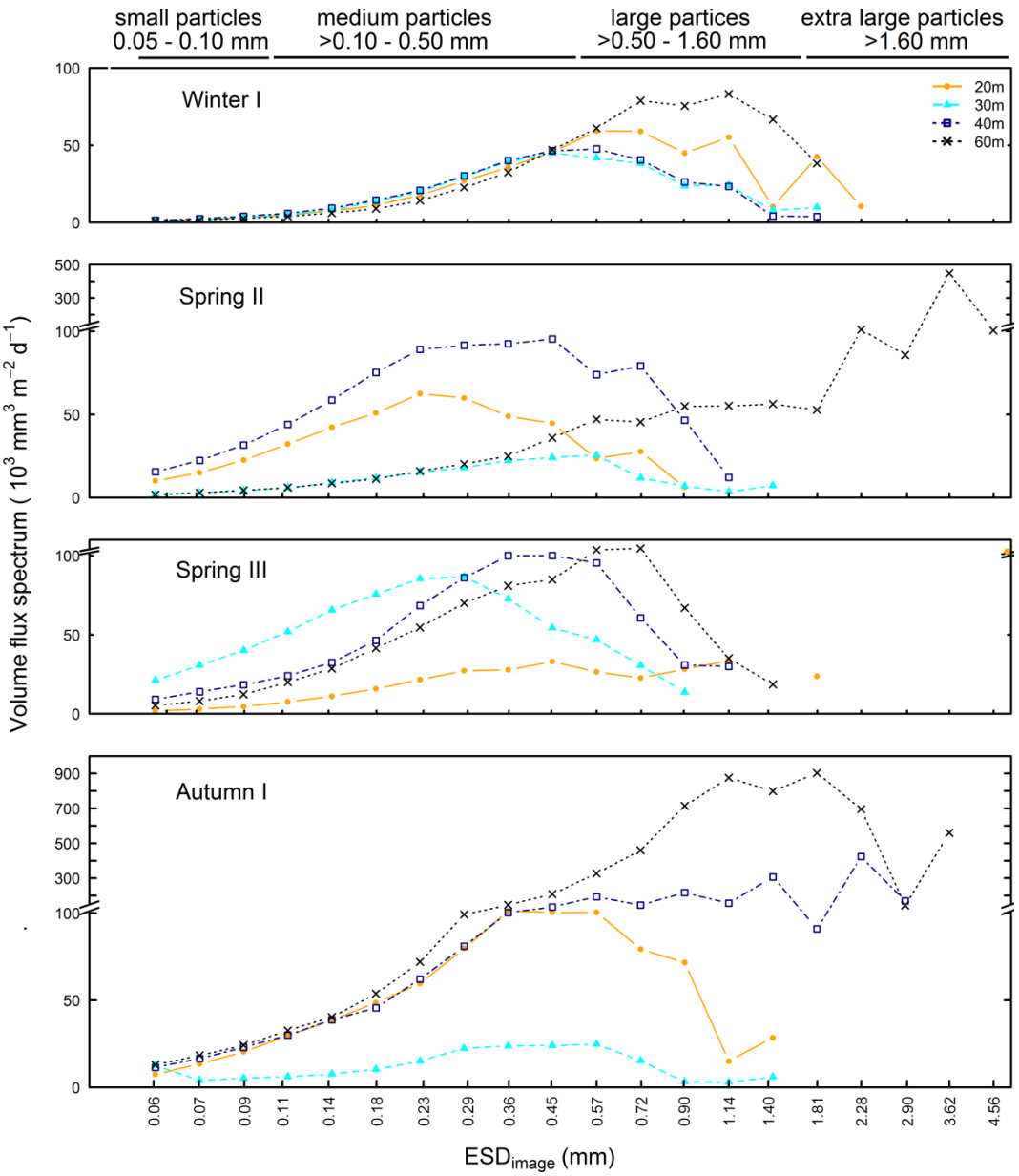

Figure 5: Volume flux spectra at the four trap deployment depths (20 m: orange solid, 30 m: turquoise stippled, 40 m: blue dotted/stippled, 60 m: black dotted) during Winter I, Spring II, Spring III, and Autumn I. The horizontal axis is logarithmic and displays the average size of the particle bins. The area under the curve reflects the total volume of particles sinking out per sampling depth, and the top line indicates the size classes of the particles. Note the broken y-axis in Spring II, Spring III and Autumn I.

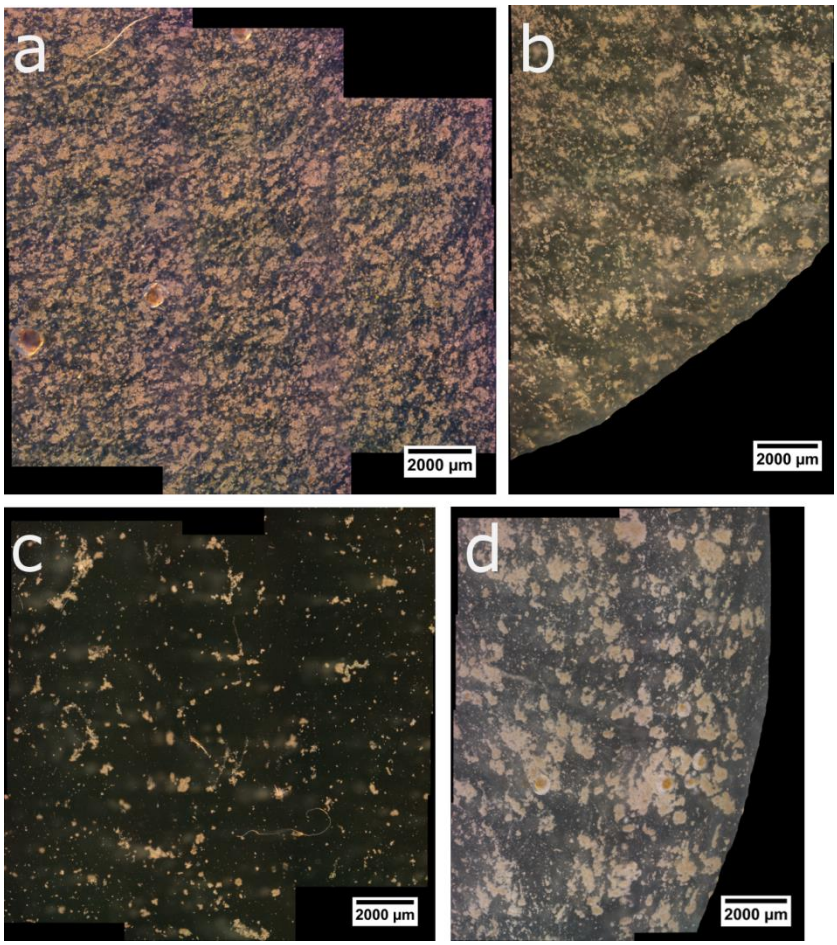

Figure 6: Example images (15 x magnification) demonstrating the different quality of sinking particles observed in the gel traps deployed at 60 m during Winter I (a), Spring II (b), Spring III (c) Autumn I (d). Note that the December sample was deployed for ~24 h, while the other samples were only deployed for ~2 h.

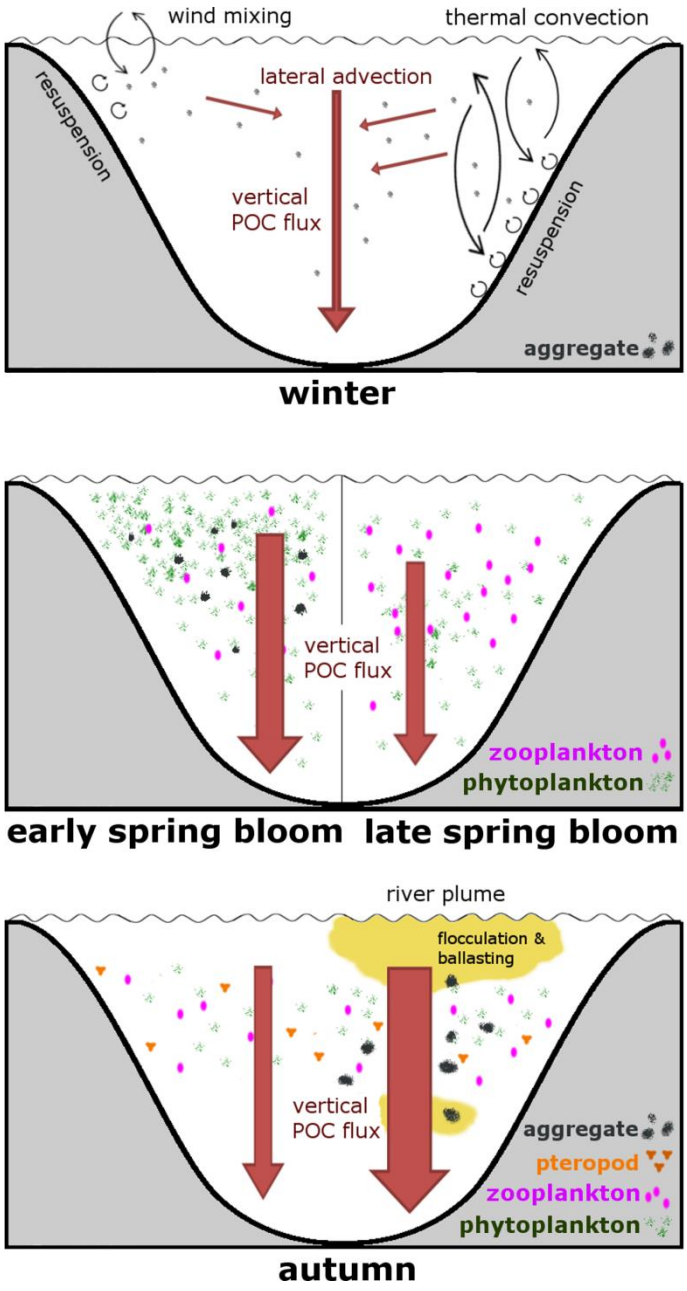

Figure 7: Conceptual model of vertical POC flux during the different seasons in the ice-free, high Arctic Adventfjorden. Resuspension of detritus from the bottom and lateral advection resulted in some vertical POC flux during winter. A strong flux event can take place during an early spring bloom situation, when aggregates of phytoplankton and detritus are formed and sink out. During a late bloom phase a stronger coupling between phytoplankton production and zooplankton diminishes the vertical POC flux. During autumn, the plume of glacial run-off can cause flocculation and aggregate formation. Entrained lithogenic material in-cooperated into sinking particles can enhance the sinking velocity of organic material, as well as high pteropod abundances.

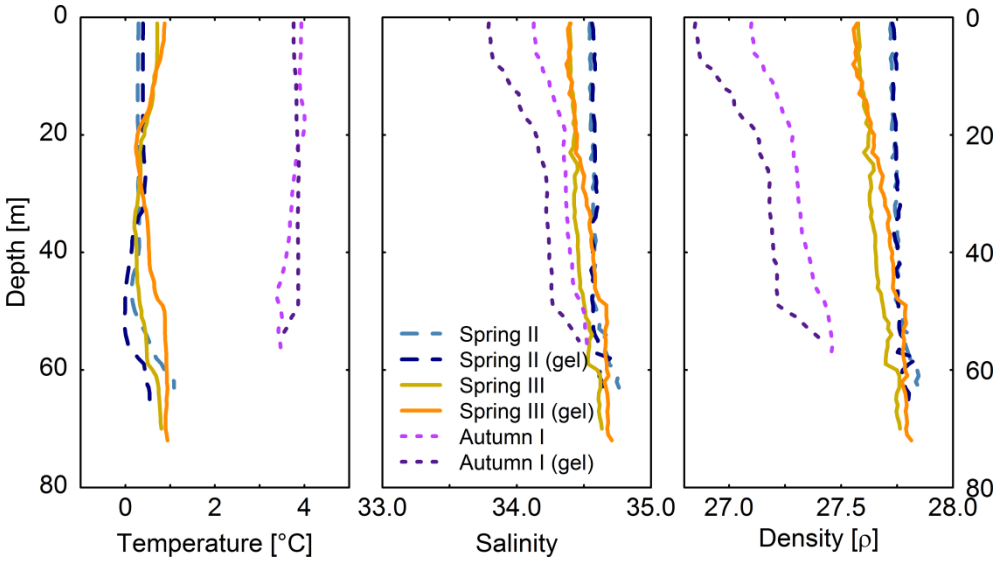

Supplement – Figure A.1: Temperature (left), salinity (middle) and density (right) plots from Spring II, Spring III and Autumn I, when CTD casts were conducted on two subsequent days (on first day, when the 24 h sediment traps array was deployed and on the second day, when the 2 h gel trap array was deployed), illustrating the variable impact of the glacial run-off on salinity during autumn.

Table 1: Sampling schedule for suspended water samples, sediment trap deployment and 'gel trap' deployment (sediment traps modified with a gel jar) at IsA station (78° 15.67' N, 15° 32.10' E). Research Vessel: 1: NorCGV Svalbard, 2: R/V Helmer Hanssen, 3: Polar Circle, 4: R/V Viking Explorer, 5: M/V Farm.

Label	Date	Boat	CTD	Euphotic zone (m)	Susp. Chl *a*, POC (mg m^{-3})	Susp. C/N	Deployment time (h)	Sediment trap** (m)	'Gel trap' (m)
Winter I	13./ 14.12.2011	1	X		5,15,25,60	5,15,25,60*	24:15	20,30,40,60	20,30,40,60
Winter II	17./ 18.01.2012	2	X		5,15,25,60	5,15,25,60	22:00	20,30,40,60	
Winter III	27./ 28.01.2012	1	X		5,15,25,60	5,15,25,60	25:00	20,30,40,60	
	09.02.2012	3	X		25				
	16.02.2012	3	X		25				
	23.02.2012	3	X		25				
	01.03.2012	3	X		25				
	08.03.2012	3			25				
	19.-22.03.2012***	3	X	34					
	29.03.2012	3	X	45	25				
	03.04.2012	3	X	40	25				
	11.04.2012	3	X	40	25				
	16.04.2012	3	X	45	25				
	23.04.2012	3	X	35	25				
Spring I	26./ 27.04.2012***	4	X	30	5,15,25,60	5,15,25,60	24:25	20,30,40,60	
	30.04.2012	3	X	30	25				
	03.05.2012	3	X	25	25				
	07.-09.05.2012***	3	X	25	25				
Spring II	10./ 11.05.2012***	4	X	25	5,15,25,60	5,15,25,60	23:25	20,30,40,60	
	11.05.2012	4					02:00		20,30,40,60
	16.05.2012	3	X						
	24.05.2012	3	X	30	25				
Spring III	30./ 31.05.2012***	4	X	20	5,15,25,60	5,15,25,60	23:45	20,30,40,60	
	31.05.2012	4					01:50		20,30,40,60
	14.06.2012	3	X		25				
	21.06.2012	3		25	25				
	06.07.2012	3	X	8	25				
	06.08.2012	3	X	30	25				
	23.08.2012	3	X	20	25				
	06.09.2012	3	X						
Autumn I	18./ 19.09.2012***	5	X	30	5,15,25,60	5,15,25,60	23:05	20,30,40,60	
	19.09.2012	5					02:30		20,30,40,60
	31.10.2012	3	X		25				

*PON samples not available
** analyzed for POC, PON and Chl *a*
*** daily sampling

Table 2: Loss rate and average sinking velocity of Chl *a* and POC.

	Winter I		**Winter II**		**Winter III**		**Spring I**		**Spring II**		**Spring III**		**Autumn I**	
	30 m	60 m	30 m	60 m	30 m	60 m	30 m	60 m	30 m	60 m	30 m	60 m	30 m	60 m
Loss rate (% d^{-1})														
- Chl *a*	9.5	5.1	9.6	8.1	6.0	8.3	-	-	15.5	7.8	19.7	9.6	6.6	3.7
- POC	6.3	5.6	6.8	5.5	6.9	4.1	13.2	8.3	7.6	5.0	5.1	2.4	36.8	21.2
Average sinking velocity (m d^{-1})														
- Chl *a*	2.8	3.1	2.8	4.6	1.7	6.6	-	-	4.2	5.6	3.8	4.2	2.4	2.8
- POC	2.0	3.7	1.6	3.0	2.0	2.6	4.6	5.6	2.7	3.9	1.6	2.2	12.0	15.7

Table 3: Quality of the sinking material denoted by the C/N ratio (PON values of Winter I not available) and the most frequent particle type (detritus = mainly small, unidentifiable particles, PP = phytoplankton, FP = fecal pellets) in the deployed gel jars. Dominant particle type in bold.

		Winter I	**Winter II**	**Winter III**	**Spring I**	**Spring II**	**Spring III**	**Autumn I**
C/N	20, 30, 40, 60 m		10.6-12.4	12.7-14.1	7.9-8.0	6.8-7.8	6.7-7.2	13.0-15.0
dominant particle type	20 m	detritus				detritus, FP	PP aggregates, detritus	**FP**, aggregates*, *Limacina* sp. (138)
	30 m	detritus, *Limacina* sp. (10)				detritus, aggregates*	PP aggregates, detritus	aggregates*, FP, *Limacina* sp. (63)
	40 m	detritus				detritus, aggregates*	aggregates*, FP	**detritus, aggregates***, FP, *Limacina* sp. (73)
	60 m	detritus, *Limacina* sp, (13)				detritus, aggregates	**FP**, aggregates*	**detritus**, aggregates, few FP, *Limacina* sp. (68)

* most likely phytoplankton aggregates

Table 4: Literature compilation of suspended POC and Chl *a* concentrations (mg m^{-3}) and the vertical flux of both parameters (mg m^{-2} d^{-1}) in high latitude fjords and the Barents Sea during winter, spring and autumn.

Place	Date	Depth (m)	Chl *a*	POC	C/N	Reference
Winter - suspended						
Adventfjorden – IsA, Svalbard	Dec 11/ Jan 12	5,15,25,60 m	<0.1	50-160	8.3-11.7	present study
Adventfjorden, Svalbard	Nov 06/ Feb 07	5,35 m	0.2-0.6	180-500	2.5-20[2]	Zajaczkowski et al. 2010
Kongsfjorden, Svalbard	Dec 06	0-50 m [1]	0.01	43	6.6	Iversen and Seuthe (2010)
Central Barents Sea	March 98	0-50 m [1]	<0.05	40-70	7.4-9.0	Olli et al. (2002)
Balsfjorden, N-Norway	Dec 08	20,63 m	0.05			Eilertsen and Degerlund (2010)
Malangen, N-Norway	Dec 08	20,417 m	0.03-0.04			Eilertsen and Degerlund (2010)
Ramfjorden, N-Norway	Nov/ Dec 89	0,10,30,50,70 m	0.03-0.20	70-270	13-25	Noji et al. (1993)
Spring - suspended						
Adventfjorden – IsA, Svalbard	Apr/ May 12	5,15,25,60 m	0.6-4.2	230-630	6.2-7.1	present study
Adventfjorden, Svalbard	Apr/ May 06	5,35 m	0.1-6.8	300-900	6-16	Zajaczkowski et al. (2010)
Kongsfjorden, Svalbard	Apr/ May 06	0-50 m [1]	0.2-10	310-670	4.6-5.3	Iversen and Seuthe (2010)
Central Barents Sea	May 98	0-50 m [1]	4.5-7.5	300-680	6.5-8.0	Olli et al. (2002)
Balsfjorden, N-Norway	Apr 92	0-36 m [1]	2.7-4.1	500-830		Reigstad et al. (1996)
Indrejord/ Tenneskjær, Malangen, N-Norway	Apr/ May 91	0-30 m [1]	0.5-2.1	410-610		Wassmann et al. (1996)
Conception Bay, Newfoundland fjord, Canada	May 98	30 m	2.5			Thompson et al. (2008)
Autumn – suspended						
Adventfjorden – IsA, Svalbard	Sept 12	5,15,25,60 m	0.3-0.4	90-130	8.5-10.5	present study
Adventfjorden, Svalbard	Oct 06	5,35 m	0.1	190-210	7.5-20 [2]	Zajaczkowski et al. (2010)
Kongsfjorden, Svalbard	Sept 06	0-50 m [1]	0.5	114	7.1	Iversen and Seuthe (2010)
Indrejord/ Tenneskjær, Malangen, N-Norway	Sept 91-Oct 91	0-30 m [1]	0.6-1.2			Wassmann et al. (1996)
Winter – sedimented						
Adventfjorden – IsA, Svalbard	Dec 11/ Jan 12	20,30,40,60 m	<0.26	90-400	10.6-14	present study
Adventfjorden, Svalbard	Nov 06/ Feb 07	35 m	0.22-0.33	500-750	6-25	Zajaczkowski et al. 2010
Central Barents Sea	March 98	30-200m[5]	<0.2	20-70		Olli et al. (2002)
Ramfjorden, N-Norway	Nov/ Dec 89	10,30,50,70 m	0.03-0.3	25-300	9-12	Noji et al. (1993)
Fanafjorden, W-Norway	Nov 79/ Feb 80	60,90 m		100-220	9-10	Wassmann (1984)
Spring – sedimented						
Adventfjorden – IsA, Svalbard	Apr/ May 12	20,30,40,60 m	2.5-20 [4]	900-1350 [4]	6.1-8.0	present study
Adventfjorden, Svalbard	Apr/ May 06	35 m	0.75-5	400-600	5-14	Zajaczkowski et al. (2010)
Central Barents Sea	May 98	30-200m[5]	10-30	200-2000		Olli et al. (2002)
Balsfjorden, N-Norway	Apr 92	30,60 m	0.5-5-5	180-630	6.5-13	Reigstad et al. (1996)

Indrejord/ Tenneskjær, Malangen, N-Norway	Apr/ May 91	30 m	0.1-13	250-750	5.5-10	Keck and Wassmann (1996)
Ullsfjorden, N-Norway	Apr 97	60 m	10-12	220-420	7.8-9.2	Reigstad et al. (2000)
Fanafjorden, W-Norway	Apr/ May 91	60,90 m		220-600	8-13	Wassmann (1984)
Conception Bay, Newfoundland fjord, Canada	May 98	40,80 m		300-700	8-9	Thompson et al. (2008)
Autumn - sedimented						
Adventfjorden – IsA, Svalbard	Sept 12	20,30,40,60 m	0.6-0.8 [4]	770-1530 [4]	13-15 [4]	present study
Adventfjorden, Svalbard	Oct 06	35 m	<0.1	500	7-16	Zajaczkowski et al. (2010)
Indrejord/ Tenneskjær, Malangen, N-Norway	Sept 91-Oct 91	30 m		130-190	7.5-8.0	Keck and Wassmann (1996)
Fanafjorden, W-Norway	Sept 80	60,90 m		300-420	9.5	Wassmann (1984)
Hudson Bay, Canada	Sept/ Oct 05	50 m	0.06-1.34	50-76.8		Lapoussière et al. (2013)

[1] Average concentration, not integrated
[2] different size fractions (0.4-2.7; 2.7-20; >20 µm)
[3] data from Reigstad and Wassmann (1996), another sampling station in the same fjord
[4] 2 h deployed traps not taken into account
[5] 30,40,50,60,90,120,150,200 m

Table A.1: Bin averages with the lower and upper limit and particle size categories, which were used to bin the particles

Bin average (mm)	Lower bin limit (mm)	Upper bin limit (mm)	Size category
0.056	0.050	0.063	
0.071	0.063	0.079	small particles
0.090	0.079	0.100	
0.113	0.100	0.126	
0.142	0.126	0.159	
0.179	0.159	0.200	
0.226	0.200	0.252	medium particles
0.285	0.252	0.318	
0.359	0.318	0.400	
0.452	0.400	0.504	
0.569	0.504	0.635	
0.717	0.635	0.800	
0.904	0.800	1.008	large particles
1.139	1.008	1.270	
1.435	1.270	1.600	
1.808	1.600	2.015	
2.278	2.015	2.539	
2.870	2.539	3.200	very large particles
3.616	3.200	4.031	
4.555	4.031	5.080	